Macromolecules

NOTE

pubs.acs.org/Macromolecules

Phase Separation of DMDBS from PP: Effect of Polymer Molecular Weight and Tacticity

K. Sreenivas, Rajeev Basargekar,† and Guruswamy Kumaraswamy*

Complex Fluids and Polymer Engineering, National Chemical Laboratory (NCL), Pune-411008, India

Supporting Information

ABSTRACT: We report an unexpected dependence of DMDBS phase separation temperature on the molecular weight of the matrix isotactic polypropylene (iPP). DMDBS crystallizes out at lower temperatures for iPP with decreasing molecular weight (and correspondingly lower tacticity). All the iPPs in our study are reasonably high molecular weight samples and there is no molecular weight dependence of their solubility parameter. Therefore, the decrease in DMDBS phase separation temperature for lower molecular weights cannot be rationalized using thermodynamic arguments. This molecular weight dependence appears to be unique to isotactic polypropylene and is not observed for either syndiotactic polypropylene or for random copolymers of isotactic polypropylene containing ethylene comonomer.

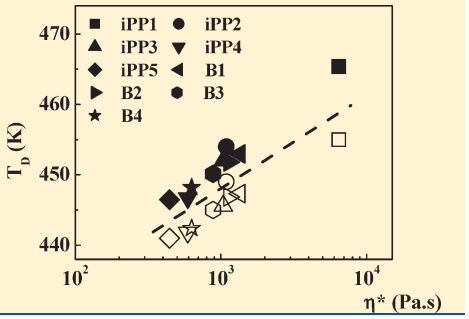

INTRODUCTION

Nucleating agents are often added to random copolymers (RCP) of isotactic polypropylene (viz. polypropylenes typically containing a few weight percent of ethylene comonomer) to increase their crystallization temperature, thereby reducing processing cycle times. Nucleating agents that enhance the transparency of the semicrystalline polymer matrix are called clarifiers. Dibenzylidene sorbitol (DBS) derivatives (such as the third generation product, 1,2,3,4-bis(3,4-dimethylbenzylidene sorbitol), DMDBS) have been extensively used in the last two decades as highly efficient clarifiers for isotactic polypropylene (iPP).[1] While sorbitol derivatives show a nucleation efficiency of only about 40% relative to self-nucleated iPP,[2,3] their efficacy as clarifiers is attributed to their extraordinary dispersibility in iPP. DMDBS dissolves in iPP melt at high temperatures (above ≈473 K), and for DMDBS concentrations between about 0.1 and 1.5% by weight, precipitates out into a network of ≈5−10 nm diameter fibrils on cooling.[4,5] Thus, the DMDBS is finely dispersed and nucleates iPP crystallization on subsequent cooling to below the iPP crystallization temperature. Molecular modeling studies suggest that sorbitol fibrils stabilize iPP chains in a helical conformation through van der Waal interactions, thereby promoting crystal nucleation.[6] However, in recent work,[7] it has been claimed that nucleation might be effected through graphoepitaxy, rather than specific chemical interactions or a lattice epitaxial match between the sorbitol and polymer crystals.

Phase separation from iPP is a function of the DMDBS concentration and the cooling rate.[5] For example, extremely slow cooling (e.g., 10 K/h) of a disk of iPP containing 1% DMDBS results in significant reduction in clarity relative to rapid cooling[5] (e.g., 10 K/min), presumably due to differences in the morphology of the phase separated DMDBS. This has consequences for manufacture and it is still a challenge to produce *clear* thick walled products by injection molding clarified iPP.[8] Imposition of flow also influences phase separation of DMDBS from iPP,[9,10] and results in oriented DMDBS networks (and, consequently, oriented polymer crystallization) and, in an increase in the DMDBS phase separation temperature. Thus, it is of interest to understand the factors that control the phase separation of DMDBS from iPP and, that influence the morphology of the phase separated DMDBS.

DBS derivatives are organogelators[3,11−14] that gel a variety of organic matrices. Intermolecular hydrogen bonding between the two hydroxyl groups on the sorbitol and π interactions that result in stacking of the bicyclo rings[15,16] result in the formation of dimers (even at DBS concentrations as low as 0.05%) that further assemble into rope-like twisted fibrillar structures. The chirality of DBS drives assembly into twisted fibers—the racemate DL-DBS does not form gels.[17] Yamasaki et al. have reported that the ratio of intermolecular to DBS-solvent hydrogen bonding determines gelation of DBS in organic solvents.[17,18] They report that DBS forms a mesh of fibrillar structures in apolar solvents, an isotropic gel phase in medium polarity solvents and spherulitic structures in polar solvents.[17,18] Thus, while solvent molecules are not incorporated into the DBS network, matrix polarity influences the morphology of DBS assembly. DBS derivatives also gel a variety of polymers apart from PP, including polyethylene terephthalate (PET), polycarbonate (PC),[19,20] polystyrene (PS),[12] polycaprolactone,[7] polyethyl methacrylate (PEMA),[21] poly(ethylene oxide) (PEO),[22] poly(propylene oxide) (PPO),[23−25] and polydimethylsiloxane (PDMS)[26] as well as graft and block copolymers.[26,27] Investigations by Spontak et al.[22,26,27] suggest that, as in organic solvents, DBS gelation in polymers too is influenced by the matrix polarity. Their

Received: January 8, 2011
Revised: February 14, 2011
Published: March 11, 2011

ACS Publications © 2011 American Chemical Society

Table 1. Characteristics of the Polymer Samples Used in Our Work[a]

sample	M_w (g mol^{-1})	PDI	η^*(Pa·s) (473 K, 1 rad·s^{-1})	isotacticity (% [*mmmm*])	⟨*m*⟩
iPP1	414700	2.6	6448	93.1	59.19
iPP2	341100	8.1	1090		
iPP3	208700	7.97	1039		
iPP4	206500	3.7	592		
iPP5	172400	4.7	444	89.6	29.20
RCP1	555300	5.9	6014		
RCP2	202400	4.6	1385		
aPP	14000	3.8	1.3	34.8	3.49
sPP1	160000	4.5	3412		
sPP2	115000	3.6	1384		
sPP3	87000	3.4	672		

[a] Molecular weights for iPP1−iPP5 and RCP1 and RCP2 were measured using a high temperature GPC with a triple detector (light scattering, viscosity and refractive index) system. These are therefore reported as absolute molecular weights. Molecular weights for aPP and sPP1−sPP3 were reported by the suppliers. The complex viscosity at 513 K for each of the samples is presented. We also present the isotacticity for iPP1, iPP5, and aPP based on high temperature NMR.

investigations[28] also demonstrate that the morphology of DBS networks phase separating from PPO block copolymers is influenced by the copolymer chain architecture (viz. PDMS-*graft*-PPO, or PDMS with telechelic PPO end-blocks), even for copolymers with comparable molecular weights and PPO fractions.

The groups of Friedrich[24,29] and Spontak[24,25] have investigated the influence of molecular weight of PPO on the phase separation of DBS. For the relatively low molecular weight PPO that they use in their investigations, there is a significant change in the polymer solubility parameter with molecular weight (up to a molecular weight of about 2000 g·mol^{-1}). Friedrich et al.[23,29] suggest that a thermodynamic Flory model (that estimates the depression in DBS phase separation temperature as a function of the difference in solubility parameters between the DBS and the polymeric matrix) can be used to rationalize the PPO molecular weight dependence on DBS phase separation temperatures. Recently,[30] phase separation of DMDBS from PP was analyzed using a similar Flory analysis and a thermodynamic phase separation temperature of 473 K was estimated for 1% DMDBS in PP. As most previous investigations[1,5,10,31,32] of DBS derivatives in iPP have used relatively high molecular weight polymers (M_w > 150000 g/mol), the sorbitol phase separation temperatures reported have been roughly similar (≈463 K, for 1% DBS concentrations). Here, we investigate the effect of varying molecular weight of matrix iPP over a wide range on the phase separation of DMDBS, and report that, surprisingly, the DMDBS phase separation temperature decreases for lower viscosity polymers. We also present data on phase separation of DMDBS from low molecular weight aPP, from random copolymers of iPP with ethylene, and from sPP of different molecular weights.

EXPERIMENTAL SECTION

The characteristics of the polymers used in our investigation are listed in Table 1. We used five homopolymer isotactic polypropylenes (iPP) and two random copolymers (RCP, containing about 3% ethylene comonomer) from Reliance Industries, India. We used atactic polypropylene (aPP) obtained from Aldrich, and three syndiotactic metallocene polypropylenes (sPP) from Fina, USA. iPP and sPP were received as pellets, while slabs of aPP were cut into small pieces. All polymers contained antioxidant stabilizers, according to information from the manufacturer. DMDBS (trade name: Millad 3988i) was obtained from Milliken and used as received. Millad 3988i contains a small amount of silica (~3%, by weight). We have performed control experiments with the neat sorbitol derivative (viz. the compounds not containing silica) to confirm that the effects reported in this work are not an artifact of the presence of silica. Polymer pellets were coated by thorough mixing with a solution of DMDBS in acetone and were compounded after solvent evaporation in a DSM corotating twin screw microcompounder (DSM-5; screw speed =100 rpm, compounding for 5 min at 493 K). Blends were prepared using the highest and lowest molecular weight iPPs (iPP1 and iPP5), as well as using iPP and aPP. The characteristics of the blends used in this work are listed in Table 2. The average tacticity reported in Table 2 is obtained as a weight-average of the tacticities of the component polymers. Tacticity and average meso sequence lengths were calculated for iPP1, iPP5, and aPP using high temperature ^{13}C NMR (experimental description, data and calculations presented in Supporting Information). We note here that the tacticity obtained for aPP is reasonably high, indicating that it is more appropriate to consider the "atactic" polypropylene as a very low isotacticity polypropylene (see Table 1). Blends were prepared by compounding the appropriate quantities of DMDBS-coated iPP and/or aPP pellets. RCP was obtained as a reactor powder and was compounded with an antioxidant and DMDBS in a twin-screw extruder. For most of the work reported here, we used a DMDBS concentration of 0.8% by weight.

Table 2. Characteristics of iPP1/iPP5 Blends as Well as iPP/aPP Blends

sample	composition	η^* (Pa·s) (473 K, 1 rad·s^{-1})	average tacticity (%)
B1	50%iPP1 + 50%iPP5	1342	91.35
B2	40%iPP1 + 60%iPP5	1138	91.00
B3	30%iPP1 + 70%iPP5	883	90.65
B4	20%iPP1 + 80%iPP5	629	90.30
C1	90%iPP1 + 10%aPP	2488	87.27
C2	75%iPP1 + 25%aPP	1090	78.53
C3	50%iPP1 + 50%aPP	511	63.95
D1	90%iPP5 + 10%aPP	484.7	84.12
D2	75%iPP5 + 25%aPP	309	75.90
D3	50%iPP5 + 50%aPP	127	62.20

We investigate phase separation of DMDBS using rheology, DSC and SAXS. Rheological measurements were performed in a 25 mm diameter

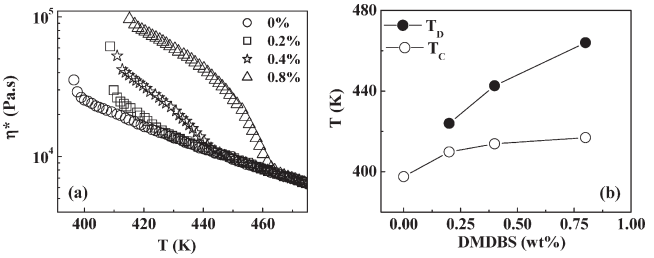

Figure 1. (a) Increase in complex viscosity (low amplitude oscillatory shear, ω = 1 rad·s^{-1}, strain =0.5%) on cooling iPP1 containing various concentrations of DMDBS. The experiment was terminated when the complex viscosity increased rapidly at low temperatures where the matrix iPP1 started to crystallize. (b) DMDBS concentration dependence of the DMDBS and polymer crystallization temperatures, obtained from rheological data, for iPP1.

parallel plate geometry on a controlled strain rheometer (ARES, TA Instruments), equipped with a forced convection oven. Samples were heated to 513 K for 5 min to ensure complete melting and were subsequently cooled at 5 K/minute while performing small amplitude oscillatory shear (ω = 1 rad/s). Experiments were conducted under nitrogen to minimize the possibility of sample degradation. All temperature ramps were repeated at least twice to check reproducibility. Frequency sweeps using small amplitude shear were performed at 513 K to characterize the samples.

DSC tests were conducted on a Q100 (TA Instruments) on thin sections (c.a. Five mg) of the samples. Samples were heated to 513 K for 2 min and subsequently cooled at 5 K/min. We present data for the cooling ramp.

SAXS measurements were made using a Bruker Nanostar (Cu K_α radiation). The Nanostar is equipped with a 18 kW rotating anode generator and a 2D multiwire detector, with a sample−detector distance of roughly 1 m. The entire X-ray flight path, including the sample chamber is evacuated to minimize air scattering. Samples were sandwiched between Kapton films and were mounted on the Bruker heating stage. 2-dimensional SAXS data was azimuthally averaged, and 1-D data is presented after background subtraction. Since the scattering from the DMDBS network is weak, we present data by subtracting the scattering at 513 K (where the DMDBS is dissolved in the molten polymer) from that at either 428 or 438 K (where the DMDBS has phase separated from the polymer).

RESULTS AND DISCUSSION

There is an exponential increase in complex viscosity, η^*, on cooling the polypropylenes from 513 K to about 473 K (see, for example, data for iPP1 in Figure 1a). The temperature dependence of η^* is approximately the same for all iPPs (and for the blends of iPP1 and iPP5) as well as for the RCPs, and corresponds to an average activation energy (averaged over the different samples) of 37.8 kJ/mol. η^* exhibits a larger thermal sensitivity for sPP, with an average activation energy (averaged over sPP1−3) of 56.7 kJ/mol. Our values for the activation energies match the values reported in the literature,[33] and are independent of molecular weight, as expected. For iPP1 (Figure 1a), we observe that, on cooling below 473 K, there is an abrupt increase in viscosity, at a temperature that depends on the concentration of the added DMDBS. For iPP1, η^* increases at about 460, 440, and 430 K for polymer containing 0.8, 0.4 and 0.2% DMDBS respectively (Figure 1a,b). All temperature ramp experiments reported here have been repeated at least twice for each sample, and the temperature for the onset of increase in η^* is

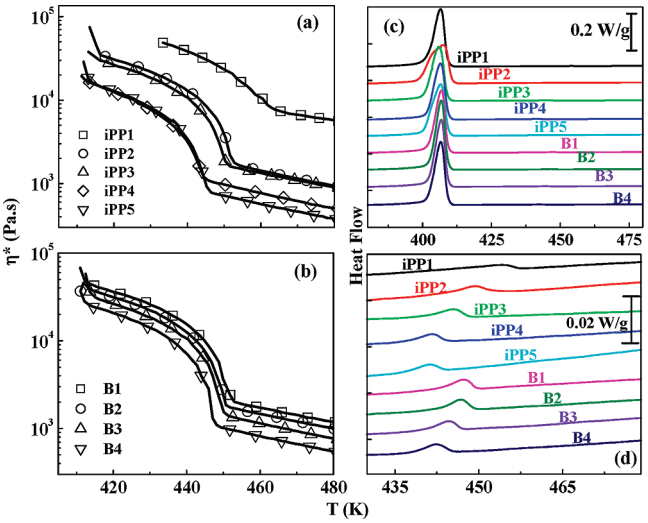

Figure 2. Increase in complex viscosity (low amplitude oscillatory shear, ω = 1 rad·s^{-1}, strain = 0.5%) on cooling (a) iPP1−iPP5 and (b) B1−B4, from the melt state. DSC cooling curves indicating the crystallization of (c) the matrix polymer and (d) DMDBS, for iPP1−iPP5 and B1−B4. Note that the enthalpy associated with crystallization of DMDBS (present at a low concentration of 0.8% in the polymer) is significantly smaller than the heat of polymer crystallization, and therefore, the DMDBS crystallization is not readily visible in part c.

reproducible to within ±1 K. Such an abrupt increase in viscosity on cooling iPP containing sorbitols has been reported in the literature[32,31] and has been demonstrated to result from crystallization of DMDBS into nanofibrils that form a network in the iPP matrix. In accord with this explanation, the magnitude of increase in η^* above that for neat iPP1, increases with DMDBS content. On cooling to lower temperatures, there is a second abrupt increase in η^* at around 410 K that corresponds to the crystallization of iPP. Addition of the nucleating agent, DMDBS, increases the polymer crystallization temperature from below 400 K for the neat iPP1 to about 410 K (Figure 1). The increase in polymer crystallization temperature is not strongly dependent on the DMDBS concentration, once it is above 0.2% (Figure 1b). The temperatures for crystallization of DMDBS and the matrix polymer from our rheology data accord with crystallization peaks from DSC experiments; and our data is in good quantitative accord with previous reports[30−32] (see Supporting Information, for similar data on other systems used in our work). In the subsequent part of this work, we examine data from systems containing 0.8% DMDBS.

We first examine the effect of iPP molecular weight on the temperature for crystallization of DMDBS (T_D) and the matrix polymer (T_C). We observe that, as the molecular weight of the matrix iPP decreases (from iPP1 to iPP5), the DMDBS crystallization temperature decreases monotonically (based on rheological experiments, Figure 2a; as well as based on DSC experiments, Figure 2d). Addition of DMDBS increases the T_C above that for the neat polymer, but this increase is not molecular weight dependent (Figure 2c). Interestingly, when we examine blends of high molecular weight polymer, iPP1, with the lower molecular weight iPP5, we observe that the crystallization temperature of DMDBS from these blends is intermediate between that for the constituent iPP1 and iPP5, and is higher with increasing fraction of iPP1 (Figure 2b,d).

dx.doi.org/10.1021/ma200035s |*Macromolecules* 2011, 44, 2358–2364

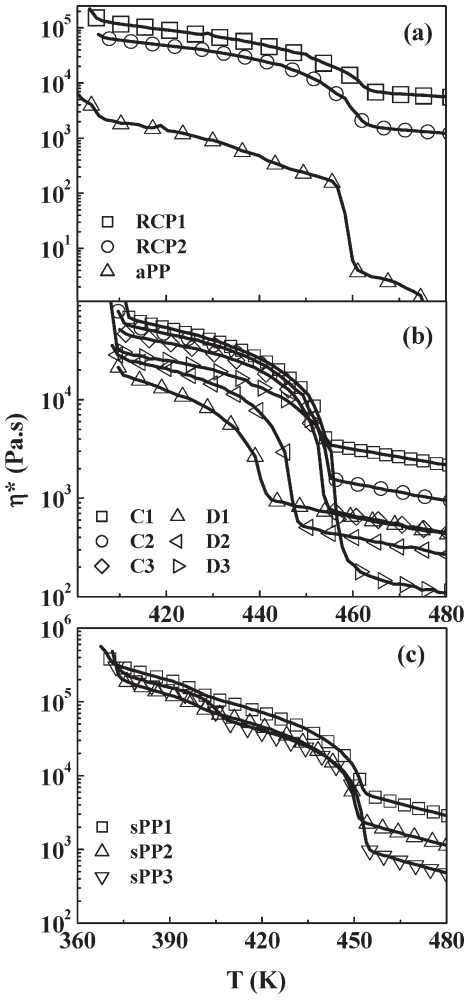

Figure 3. Increase in complex viscosity (low amplitude oscillatory shear, ω = 1 rad·s^{-1}, strain = 0.5%) on cooling (a) RCP1, RCP2, and aPP, (b) C1−C3 and D1−D3, and (c) sPP1−sPP3.

The DMDBS crystallization temperature is also obtained from rheological and DSC experiments for polypropylene random copolymers (RCP1 and RCP2; rheological data shown in Figure 3 a; DSC data in Supporting Information), atactic polypropylene (aPP, Figure 3a), for blends of iPP1 with aPP (C1−3) and of iPP5 with aPP (D1−3, Figure 3b) as well as for three syndiotactic PPs with different molecular weights (sPP1−3, Figure 3c). For all these polypropylene samples with different molecular weights and tacticities, crystallization of DMDBS results in an increase in η^* at a well-defined onset temperature, T_D. We combine all this data to examine the influence of polymer molecular weight and tacticity on T_D (Figure 4).

iPP1−5 are commercial isotactic polypropylenes. Therefore, they have a broad distribution of molar mass (see Table 1, and GPC in Supporting Information). For ease of comparison between samples with different M_W and PDI, we present data on T_D as a function of the complex viscosity of the polymer matrix. As the viscosity of the polymer matrix scales nonlinearly with the polymer molecular weight,[34] η^* is biased toward higher moments of the molecular weight distribution. For iPP1−5 and for blends of iPP1 and iPP5 (viz. B1−4), we observe that there is a monotonic decrease in T_D with decrease in the matrix viscosity (η^* at 200 °C, ω = 1 rad·s^{-1}, Figure 4a). We observe that T_D decreases with decrease in ln(η^*) (by about 14 K over a 10-fold change in η^*), for the range of molecular weights considered in our work (Figure 4a). We observe the same trends for T_D from two independent experimental techniques, viz. rheology and DSC (Figure 4a). In both rheology and DSC experiments, the sample was cooled at the same rate, viz. 5 K/min. However, the value of T_D from the *onset* of increase in η^* in our rheology experiments is typically about 4−5 K higher than the *peak* temperature from DSC experiments (as is evident in Figure 4a). This difference is probably indicative of the different sensitivities of the two techniques to DMDBS crystallization and network formation. As two independent experimental techniques, rheology and DSC indicate that the decrease in T_D correlates with the viscosity of the matrix polymer, we focus on the trends observed for T_D, rather than specific values, and examine T_D from rheological measurements for the other polymers.

High temperature solution ^{13}C NMR data (see Table 1, and Supporting Information) indicates that iPP1 (the highest molecular weight iPP) has a higher average isotacticity compared with iPP5. iPP1−5 are all produced using the same fluidized bed reactor (viz. gas phase process) and Ziegler−Natta titanium catalyst technology, where molecular weight control is achieved by injection of hydrogen in the reactor, as a chain transfer agent. The correlation between molecular weight and isotacticity in such materials is not surprising.[35,36] Therefore, it is not clear whether the change in T_D for iPP1−5 and B1−4 is correlated with the change in η^* or the change in isotacticity. To investigate this, we examine the trends in T_D for the other polypropylenes.

DMDBS crystallization from aPP (that has a very low viscosity compared with iPP1−5, corresponding to a low molecular weight, see Table 1) is observed to happen at $T_D \approx$ 460 K, comparable to that for iPP1 (Figure 4b). This is surprising when compared to our iPP data: aPP, a low molecular weight, very low isotacticity polypropylene has a relatively high T_D. Thus, it appears that the change in T_D cannot be correlated with only the η^* (or molecular weight) or only the isotacticity of the polypropylenes. To investigate this point in more detail, we now consider blends of aPP and iPP. aPP and iPP are completely miscible in all proportions.[33] Therefore, we can vary the *average* tacticity by blending iPP and aPP. When we examine C1−3 (blends of iPP1 with aPP), and D1−3 (blends of iPP5 with aPP), we observe a large scatter in the observed T_D (Figure 4c). A comparison of C3 and D1 (approximately similar η^*, but widely different average isotacticities), and of C1 and D1 (approximately similar average isotacticity, but widely different η^*) reinforces our conclusion that T_D does not correlate specifically with either the average tacticity or the average viscosity (viz. molecular weight) of the matrix polymer. Furthermore, we also observe no correlation of T_D with polypropylene viscosity (and therefore, molecular weight) for RCPs (Figure 4b). Both RCP1 and RCP2 exhibit a similar T_D, comparable to that for aPP and iPP1. Finally, we observe that there is no significant dependence of T_D on sPP molecular weight (Figure 4 b). Therefore, the correlation between T_D and polymer viscosity (and therefore molecular weight) appears to be specific to iPPs, for samples where most chains in the sample have a reasonably high isotacticity.

We now examine the effect of molecular weight and tacticity on the structure of the nanofibers formed by crystallization of DMDBS on cooling. We examine small angle scattering of X-rays from selected samples (iPP1, iPP5, aPP, and sPP1) cooled to a

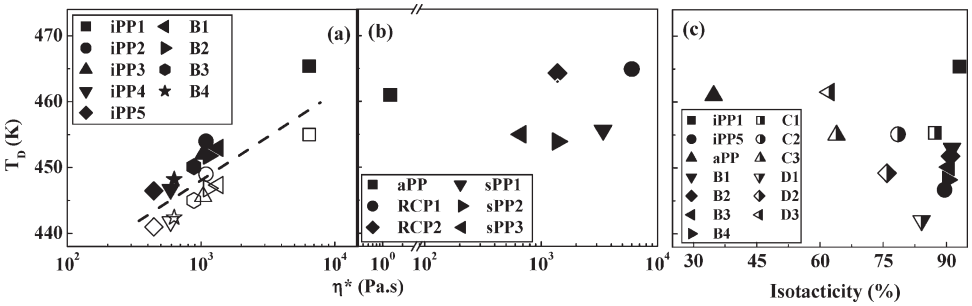

Figure 4. (a) Summary of the DMDBS crystallization temperatures from rheological measurements (filled symbols) and DSC (open symbols) for iPP1−iPP5 and B1−B5. The line is shown as a guide to the eye and does not represent a fit to the data. (b) Comparison of the DMDBS crystallization temperatures from aPP, RCP1, RCP2 and from sPP1−sPP3. (c) Comparison of the DMDBS crystallization temperatures for iPP1/iPP5 blends (B1−B4) and for the iPP/aPP blends (C1−C3 and D1−D3).

temperature $T. < T_D$, where our rheology and DSC data indicate that DMDBS has crystallized to form a network (Figure 4). We initially investigated scattering at 428 K, and observed that the scattered intensity increases with time over a period of several hours for iPP1 and iPP5, but not for aPP or sPP. This time-dependent increase in scattered intensity from iPP-DMDBS systems has been reported in the literature[30] and has been attributed to growth of the DMDBS nanofibers. However, in our experiments, we observe that the increase in scattering intensity for iPP1 and iPP5 with time correlates with the appearance of a scattering peak around q = 0.04 Å^{-1} (Supporting Information. The scattering peak at q = 0.04 Å^{-1} is apparent only when the scattered intensity is plotted on a logarithmic scale). This peak corresponds to the lamellar long spacing from iPP crystallization (confirmed by examining room temperature SAXS from these systems, where the scattering is dominated by the structure factor peak from the correlations between crystalline lamellar stacks). Therefore, we believe that the increase in scattered intensity for iPP1 and iPP5 can be attributed to crystallization of the matrix iPP on the DMDBS nanofibers. While crystallization of iPP at such high temperatures is unexpected, it is not unprecedented—crystallization of iPP on flow-induced crystallization nuclei has been observed at temperatures as high as 441 K.[37] DMDBS nanofibers, however, appear to be unable to nucleate iPP crystallization at higher temperatures and we observe no increase in scattering intensity with time from iPP1 at 438 K (Supporting Information). As T_C for sPP1 is lower than that for the iPPs, and since aPP is not very crystallizable, we observe no increase in scattering intensity from these systems at 428 K. Interestingly, for scattering from iPP1 at 428 K, for t = 0 (viz. scattering data collected in the first 20 min after cooling to 428 K, before iPP1 has crystallized to a significant extent), the scattered intensity from the DMDBS is similar that at 438 K (see Supporting Information). Therefore, it appears that the structure formed by the DMDBS as it crystallizes out from the polymer melt does not change on cooling to lower temperatures. Therefore, here we present data for scattering on cooling to T = 438 K, where the DMDBS has crystallized out of the polymer (see Figure 4), but where the matrix polypropylene does not crystallize.

As DMDBS is present in a small concentration (0.8%, by weight), we examine the scattering from the DMDBS nanofibers by subtracting the scattered intensity at 513 K (where the DMDBS is dissolved in the polypropylene, viz. the "matrix" scattering intensity) from that at 428 K ($<T_D$), as suggested in the literature.[31] At low q, the (matrix subtracted) scattered

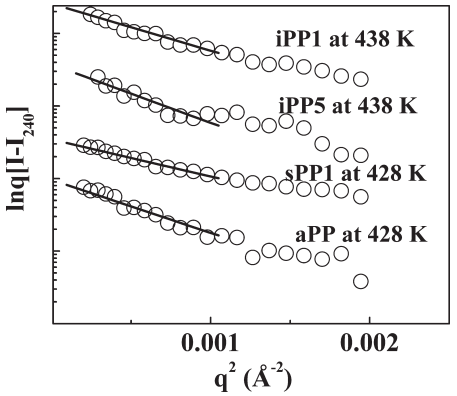

Figure 5. Intensity of scattered X-rays from iPP1, iPP5 (both at 438 K), aPP and sPP1 (both at 428 K) containing 0.8% DMDBS, plotted after subtracting the scattering at high temperature (513 K), as explained in the text. Data is presented as a Guinier plot and we show ln(qI) versus q^2 for low q. The plots are vertically shifted for ease of viewing.

intensity, I, shows a linear region in a Guinier plot of ln(qI) versus q^2, for all the polypropylene samples investigated (Figure 5), suggesting that the scattering entities, viz. the crystalline DMDBS forms one-dimensional nanofibers, as expected from literature reports. We can obtain the radius of the DMDBS nanofiber, $R = R_g/\sqrt{2}$, from the slope of the scattered intensity in the Guinier region, as follows.[38]

$$R = \sqrt{(4^*\{\text{slope of } \ln(qI) \text{ versus } q^2\}} \qquad (1)$$

Our analysis yields a radius for the DMDBS nanofibers of 7.7, 5.3, 7.3, and 9.2 nm in iPP1, iPP5, sPP1, and aPP matrices, respectively. Since the DMDBS nanofibers scatter only weakly, we do not believe that the differences in fiber radii obtained are significant enough to merit detailed discussion. Thus, our SAXS analysis confirms that the behavior of DMDBS is not qualitatively different, as it crystallizes out of iPP, aPP and sPP. For all the polypropylenes (iPP, aPP and sPP) investigated here, the DMDBS crystallizes into a nanofibrillar morphology, with nanofibers of radius approximately between 5 and 10 nm.

Finally, we return to a discussion of the trends in T_D. Our data clearly indicate a correlation between T_D and the viscosity for iPP. An increase in T_D with molecular weight has been reported[23−25,29] for relatively low molecular weight PPOs. These are polar polymers, and, for the low molecular weight materials examined in previous work, there is a significant effect of end

dx.doi.org/10.1021/ma200035s |Macromolecules 2011, 44, 2358–2364

groups on the polymer solubility parameter. Thus, the change in T_D has been rationalized using a thermodynamic argument that considers the molecular weight dependence of the matrix PPO, on the difference in solubility parameters between the DMDBS and the PPO. In contrast with previous investigations, the iPPs used in our experiments are all relatively high molecular weight apolar polymers, and we do not expect any significant change in the polymer solubility parameter with molecular weight.[39−42] Interestingly, we note that the Flory argument has been used[30] to estimate an equilibrium DMDBS crystallization temperature of about 473 K (for a DMDBS concentration of 1% in iPP). Thus, the equilibrium DMDBS crystallization temperature is closer to the experimental T_D values for iPP1, aPP and the RCPs (∼465 K), as compared to the values for the lower molecular weight iPPs. As we did not have access to higher molecular weight iPPs, we could not determine if, as expected, there is a plateau in T_D at high matrix molecular weights. Thus, it appears that it is specifically the low molecular weight iPPs that demonstrate an unusual reduction in T_D (when compared with the high molecular weight iPPs, where T_D accords with the literature reports). This decrease in T_D with decreasing molecular weight is highly unusual, and cannot be rationalized based on current theories. Molecular modeling indicates that DMDBS molecules dimerize in apolar matrices, and that the cleft in the butterfly shaped DMDBS dimers interact with the helices formed as iPP is cooled. It is possible that an influence of iPP molecular weight on helix formation during cooling might result in the observed decrease in T_D with decreasing iPP molecular weight. Preliminary FTIR experiments to verify this were inconclusive since it is difficult to quantitatively compare time-dependent FTIR from crystallizing iPP samples. Thus, a definitive explanation for the reduction in T_D for the low molecular weight iPPs is currently elusive.

Why is there no matrix molecular weight dependence of T_D for RCPs? We suggest the following speculative argument. For Ziegler−Natta iPPs, the stereoregularity of the chains is known to be correlated to the molecular weight.[35] Thus, not only do iPP1−5 have a broad molecular weight distribution, they are also compositionally heterogeneous with the high molecular weight chains within the distribution having higher stereoregularity as compared to the low molecular weight chains. However, for iPPs produced using titanium catalysts with optimized donor systems, similar to those used in our work, the isotacticity for even the low molecular weight chains in the distribution has been shown[35] to be ∼60 to 70% (compare with 33% for aPP, Table 1). Thus, all the chains in an iPP can be considered to have a reasonably high isotacticity. In contrast, for RCPs produced using the same fluidized bed process and the same catalyst chemistry, the meso sequences in the polymer chains are interrupted by incorporation of comonomer ethylene. Thus, while RCPs too are expected to exhibit compositional heterogeneity that is correlated with molecular weight,[36,43] the average meso sequence lengths in RCPs are smaller than in iPPs.

In preliminary experiments to validate this hypothesis, we fractionated iPP5 and RCP1 into two fractions based on their solubility (see Supporting Information for experimental details). It is reasonable to assume that solubility correlates with crystallizability, and therefore, with the tacticity for iPP (or comonomer ethylene content for the RCP). For both iPP5 and RCP1, the dissolved fraction has a lower viscosity (by about 2-fold) as compared to the undissolved fraction, indicating that the dissolved fraction has a lower molecular weight. Thus, fractionation divides the polymers into a low molecular weight part (that has lower tacticity and higher comonomer content) and a high molecular weight part (with higher tacticity and lower comonomer content). We adjust the dissolution temperatures such that the dissolved fraction is about 30−40% of the total, and note that, as expected, a significantly lower temperature is required to achieve this for RCP1 (368 K) as compared to iPP5 (383 K). Both dissolved and undissolved fractions of iPP5 show significantly higher heats of fusion (ΔH_m = 124 J/g and 133 J/g, respectively) when compared with the corresponding RCP1 fractions (ΔH_m = 93 J/g and 99 J/g, respectively). Interestingly, we observe that the high molecular weight/higher tacticity fraction of iPP5 shows a higher T_D (=463 K) relative to the low molecular weight/low tacticity fraction (T_D = 458 K). However, both fractions of RCP1 have roughly the same T_D (≈467 K). Thus, even for the undissolved RCP fraction (viz. the high molecular weight, lower ethylene content fraction with the higher heat of fusion), the ethylene incorporation is high enough to not influence the DMDBS T_D. Thus, our experiments suggest that the correlation between T_D and molecular characteristics (molecular weight and tacticity) holds only for reasonably isotactic iPPs.

SUMMARY

We observe that the phase separation temperature of DMDBS from isotactic polypropylene shows an unusual dependence on the molecular weight of the matrix polymer. The phase separation temperature of DMDBS decreases by about 14 K for a 10-fold decrease in polymer viscosity (corresponding to an approximately 2-fold reduction in polymer molecular weight). This molecular weight dependence of the DMDBS phase separation temperature is observed only for isotactic polypropylene. Atactic polypropylene, syndiotactic polypropylene and propylene−ethylene copolymers do not exhibit this effect. The specific interactions between low molecular weight isotactic polypropylene and DMDBS that result in the observed decrease in the phase separation temperature of DMDBS are not yet understood.

ASSOCIATED CONTENT

Supporting Information. Characterization data (GPC, NMR, DSC) for the polymers used in this work, as well as SAXS data. This material is available free of charge via the Internet at http://pubs.acs.org.

AUTHOR INFORMATION

Corresponding Author

*Telephone: +91-20-2590-2182. Fax: +91-20-2590-2618. E-mail: g.kumaraswamy@ncl.res.in.

Present Addresses

[†]Reliance Technology Group, Reliance Industries Limited, Mumbai, India.

ACKNOWLEDGMENT

We acknowledge Dr. P. R. Rajamohanan for performing the high temperature ^{13}C NMR experiments, and Mrs. Deepa Dhoble for help in the high temperature GPC experiments. We are very grateful to Dr. T. P. Mohandas for helpful discussions to interpret the ^{13}C NMR.

REFERENCES

(1) Marco, C.; Ellis, G.; Gomez, M. A.; Arribas, J. M. *J. Appl. Polym. Sci.* **2002**, *84*, 2440–2450.
(2) Fillon, B.; Lotz, B.; Thierry, A.; Wittmann, J. C. *J. Polym. Sci., Part B: Polym. Phys.* **1993**, *31*, 1395–1405.
(3) Thierry, A.; Fillon, B.; Straup, C.; Lotz, B.; Wittmann, J. C. *Prog. Colloid Polym. Sci.* **1992**, *87*, 28–31.
(4) Thierry, A.; Straupe, C.; Lotz, B.; Wittmann, J. C. *Polym. Commun.* **1990**, *31*, 299–301.
(5) Kristiansen, M.; Werner, M.; Tervoort, T.; Smith, P. *Macromolecules* **2003**, *36*, 5150–5156.
(6) Smith, T. L.; Masilamani, D.; Bui, L. K.; Khanna, Y. P.; Bray, R. G.; Hammond, W. B.; Curran, S.; Belles, J. J., Jr.; Binder-Castellit, S. *Macromolecules* **1994**, *27*, 3147–3155.
(7) Siripitayananon, J.; Wangsoub, S.; Olley, R. H.; Mitchell, G. R. *Macromol. Rapid Commun.* **2004**, *25*, 1365–1370.
(8) Tenma, M.; Yamaguchi, M. *Polym. Eng. Sci.* **2007**, *47*, 1441–1446.
(9) Nogales, A.; Olley, R. H.; Mitchell, G. R. *Macromol. Rapid Commun.* **2003**, *24*, 496–502.
(10) Sreenivas, K.; Pol, H. V.; Kumaraswamy, G. *Polym. Eng. Sci.* **2010**July, in press.
(11) Balzano, L.; Portale, G.; Peters, G. W. M.; Rastogi, S. *Macromolecules* **2008**, *41*, 5350–5355.
(12) Lipp, J.; Shuster, M.; Feldman, G.; Cohen, Y. *Macromolecules* **2008**, *41*, 136–140.
(13) Terech, P.; Weiss, R. G. *Chem. Rev.* **1997**, *97*, 3133–3159.
(14) Thierry, A.; Straupe, C.; Wittmann, J.-C.; Lotz, B. *Macromol. Symp.* **2006**, *241*, 103–110.
(15) Watase, M.; Nakatani, Y.; Itagaki, H. *J. Phys. Chem. B* **1999**, *103*, 2366–2373.
(16) Wilder, E. A.; Spontak, R. J.; Hall, C. K. *Molecul. Phys.* **2003**, *101*, 3017–3027.
(17) Yamasaki, S.; Ohashi, Y.; Tsutsumi, H.; Tsujii, K. *Bull. Chem. Soc. Jpn.* **1995**, *68*, 146–151.
(18) Yamasaki, S.; Tsutsumi, H. *Bull. Chem. Soc. Jpn.* **1995**, *68*, 123–127.
(19) Mitra, D.; Misra, A. *J. Appl. Polym. Sci.* **1988**, *36*, 387.
(20) Mitra, D.; Misra, A. *Polymer* **1988**, *29*, 1990.
(21) Wilder, E. A.; Braunfeld, M. B.; Jinnai, H.; Hall, C. K.; Agard, D. A.; Spontak, R. J. *J. Phys. Chem. B* **2003**, *107*, 11633–11642.
(22) Wilder, E. A.; Hall, C. K.; Khan, S. A.; Spontak, R. J. *Langmuir* **2003**, *19*, 6004–6013.
(23) Frassdorf, W.; Fahrländer, M.; Fuchs, K.; Friedrich, a. C. *J. Rheol.* **2003**, *47*, 1445–1454.
(24) Mercurio, D. J.; Khan, S. A.; Spontak, R. J. *Rheol. Acta* **2001**, *40*, 30–38.
(25) Mercurio, D. J.; Spontak, R. J. *J. Phys. Chem. B* **2001**, *105*, 2091–2098.
(26) Ilzhoefer, J. R.; Spontak, R. J. *Langmuir* **1995**, *11*, 3288–3291.
(27) Wilder, E. A.; Hall, C. K.; Spontak, a. R. J. *J. Colloid Interface Sci.* **2003**, *267*, 509–518.
(28) Nunez, C. M.; Whitfield, J. K.; Mercurio, D. J.; Ilzhoefer, J. R.; J. Spontak, R.; Khan, S. A. *Macromol. Symp.* **1996**, *106*, 275–286.
(29) Fahrlander, M.; Fuchs, K.; Friedrich, C. *J. Rheol.* **2000**, *44*, 1103–1119.
(30) Lipp, J.; Shuster, M.; Terry, A. E.; Cohen, Y. *Langmuir* **2006**, *22*, 6398–6402.
(31) Balzano, L.; Rastogi, S.; Peters, G. W. M. *Macromolecules* **2008**, *41*, 399–408.
(32) Shepard, T. A.; Delsorbo, C. R.; Louth, R. M.; Walborn, O. L.; Norman, D. A.; Harvey, N. G.; Richarad, J. S. *Polym. Sci., part:B: Polym. Phys.* **1997**, *35*, 2617–2628.
(33) Eckstein, A.; Suhm, J.; Friedrich, C.; Maier, R.-D.; Sassmannshausen, J.; Bochmann, M.; Mulhaupt, R. *Macromolecules* **1998**, *31*, 1335–1340.
(34) Gennes, P.-G., *Scaling Concepts in Polymer Physics*, 1st ed.; Cornell University Press: Ithaca, NY, 1979.
(35) Paukkeri, R.; Vaananen, T.; Lehtinen, A. *Polymer* **1993**, *34*, 2488–2494.
(36) Soares, J. B. P.; Hamielec, A. E. *Polymer* **1995**, *36*, 1639–1654.
(37) Kumaraswamy, G.; Kornfield, J. A.; Yeh, F.; Hsiao, B. S. *Macromolecules* **2002**, *35*, 1762–1769.
(38) Guinier, A.; Fournet, G., *Small-Angle Scattering of X-rays.*: Wiley: New York, 1955.
(39) Huang, J.-C. *J. Appl. Polym. Sci.* **2009**, *112*, 2027–2032.
(40) Maier, R.-D.; Thomann, R.; Kressler, J.; Mulhapt, R.; Rudolf, B. *J. Polym. Sci., B: Polym Phys* **1997**, *35*, 1135–1144.
(41) Michaels, A. S.; Vieth, W. R.; Alcalay, H. H. *J. Appl. Polym. Sci.* **1968**, *12*, 1621–1624.
(42) Rojo, E.; Fernandez, M.; Munoz, M. E.; Santamarıa, A. *Polymer* **2006**, *47*, 7853–7858.
(43) Zhang, Y.-D.; Wu, C.-J.; Zhu, S.-N. *Polym. J.* **2002**, *34*, 700–708.